EIGENFREQUENCY BASED SENSITIVITY ANALYSIS OF VEHICLE DRIVETRAIN OSCILLATIONS

Oliver Manuel Krieg[a], Jens Neumann[b], Bernhard Hoess[c], Heinz Ulbrich[d]

[a] BMW Group Research and Technology, Hanauer Str. 46, 80992 Munich, Germany
[b] BMW AG, Hufelandstr. 4, 80788 Munich, Germany
[c] BMW Group Research and Technology, Hanauer Str. 46, 80992 Munich, Germany
[d] Institute of Applied Mechanics, Technical University of Munich, Boltzmannstraße 15, 85748 Garching, Germany

[a]Oliver.M.Krieg@bmw.de, [b]Jens.JE.Neumann@bmw.de, [c]Bernhard.Hoess@bmw.de, [d]Ulbrich@amm.mw.tu-muenchen.de

ABSTRACT

For vehicle drivetrain design, there is a serious conflict of objectives between the oscillation phenomena shuffle and cyclic irregularities. The purpose of this paper is to illustrate a methodology to analyse and visualise the sensitivities of drivetrain eigenfrequencies in order to solve this conflict of objectives for the drivetrain design process for selected vehicle drivetrain concepts. Starting with a complex and detailed non-linear model, different simplifications are performed to finally visualise the sensitivities of relevant eigenfrequencies. This provides a profound understanding of the dynamic behaviour of the vehicle and enables engineers to identify parameter combinations that solve or palliate this conflict of objectives. Two exemplary measures are derived and the palliation effect is examined with the complex simulation models.

Keywords: sensitivity, vehicle transient behaviour, eigenfrequency, oscillations

1. INTRODUCTION

Due to the increasing CO_2 requirements of the vehicle fleet consumption, there is a considerable trend of vehicle manufacturers to optimize the vehicle fuel economy. Nevertheless, there is a serious conflict of objectives for the design of vehicle drivetrains due to the fact that vehicle dynamics and comfort aspects also have to be taken into account. Therefore, the vehicle performance needs to meet the requirements and perturbing oscillations must not exceed an admissible threshold.

In order to predict the behaviour of a future vehicle, complex non-linear models are used for the simulation of different components and settings. The pure implementation of a complex model however is not sufficient to gain a parameter setup that meets the requirements. The mere amount of parameters often prevents a straight-forward approach by simply adjusting one parameter after the other to approximate a good setup.

Understanding and visualising the relevant sensitivities can seriously improve the design process since it helps identifying parameters that approximate good vehicle setups, gives profound understanding of the dynamics of the system and facilitates solutions for the described conflicts of objectives. Furthermore, no optimisation algorithms are needed, which usually require distinct optimisation criteria and boundaries that often do not exist explicitly, and will not necessarily lead to an improved understanding of the dynamics of the system. A methodology is presented in this paper performing different simplifications, analysing eigenfrequency sensitivities based on (Dresig and Holzweißig 2010) and deriving measures to palliate the conflict of objectives for shuffle and cyclic irregularity for low frequencies for the vehicle drivetrain design process.

Numerous works are concerned with the discussed oscillation phenomena of a vehicle drivetrain. A complete overview would go beyond the scope of this paper. Therefore only selected works are presented here. In (Bencker 1998), experimental and simulative studies on shuffle are performed to identify palliative measures for the drivetrain. An analysis of a different engine torque excitation for shuffle follows in (Hülsmann 2007). Various works are concerned with active control of shuffle, e.g. (Best 1998), (Lefebvre, Chevrel, and Richard 2003), (Richard, Chevrel, and Maillard 1999). A holistic analysis of driveline oscillations due to cyclic irregularity is presented in (Gosdin 1985). Here, a parameter optimisation is achieved for the vehicle driveline for predefined boundaries. Various works are concerned with mechanical, semi-active or active components reducing cyclic irregularity, e.g. (Reik, Fidlin, and Seebacher 2009). New components for palliation as well as active control algorithm for shuffle control can both profit from the presented methodology. For the former, the discussed conflict of objectives is still present and any palliation helps the effectiveness of an additional

drivetrain component. For the latter, improved shuffle behaviour reduces the control requirements.

Starting point is a detailed model based on the physical behaviour of the different elements of the drivetrain. This model including measurement comparisons is presented in Section 2. The desired vehicle behaviour and existing conflicts of objectives are described in Section 3. In Section 4, different model simplifications are derived and the eigenfrequency sensitivity analysis is performed. The results of the presented methodology are then used to identify palliative measures for the behaviour of a three cylinder drivetrain, which is derived from the six cylinder drivetrain from Section 2. Finally, the results are summarised in Section 5.

2. DRIVETRAIN MODELLING

The examined prototype vehicle is a vehicle fitted with a six cylinder turbocharged engine. First, the engine model is presented, followed by the mechanical drivetrain model. Finally a measurement comparison is illustrated in this section.

2.1. Thermodynamic Engine Implementation

The cylinder volume is the core element of the engine model. Here, the combustion takes place and the mechanical work is transferred to the crank drive. It is basically a homogeneous volume following the first law of thermodynamics applied to open systems (Müller and Müller 2005):

$$\dot{U} = \dot{Q} + \dot{E} + \dot{W} \qquad (1)$$

Here, $\dot{U}$ represents the first derivate of the internal energy with respect to time, $\dot{Q}$ the heat flow and $\dot{W}$ the mechanical power done on the system. $\dot{E}$ represents the inner energy flow of matter entering and leaving the system.

The conservation of mass and the caloric theory corresponding to the cylinder gases must also be taken into account for the model. Additional components as valves, a combustion model, heat transfer elements or the crank drive are also required to model the physical behaviour of the engine. A possible implementation of these elements is described in (Krieg, Förg, and Ulbrich 2011).

Deviant from the filling and emptying approach presented in (Krieg, Förg, and Ulbrich 2011), the fluid oscillations of the intake and exhaust manifold are also considered here. Intake and exhaust manifold are modelled as sequence of pipes, which are discretised homogenous volumes. Incorporating detailed intake and exhaust manifold models can increase the quality of the simulation results for certain operating conditions but leads to more complex models and longer simulation duration. The implementation of these pipes follows the conservation of mass and energy and, in addition to the

filling and emptying approach, also the conservation of linear momentum:

$$\frac{\partial}{\partial t}(\rho A \omega) + \frac{\partial}{\partial x}(\rho A \omega^2) + \frac{\partial}{\partial x}(p A) = -\rho A k_f \qquad (2)$$

Here, ρ represents fluid density, A the pipe cross section area, ω the fluid velocity and p the fluid pressure. Furthermore, t represents time, x position and k_f is a coefficient for friction. A solution for the partial differential equation requires a discretisation method, e.g. the finite volume method (Dick 2009). A possible implementation of the pipes is presented in (Miersch 2003). Components implemented as characteristic maps and not physically are the turbine and the compressor of the turbocharger. Here, the mass flow is estimated according to the turbocharger shaft speed and the fluid pressure of the incoming and outgoing pipes of these components, as derived from measured data. The implementation of turbochargers is described e.g. in (Baines and Fredriksson 2007).

2.2. Mechanical Drivetrain Implementation

For the engine crank drive model, an analytical and a multibody approach are possible implementations. A deduction of an analytical implementation according to the projective Newton-Euler equations and an evaluation of both implementation approaches is presented in (Krieg, Förg, and Ulbrich 2011).

All shafts of the drivetrain are modelled as rotational inertias and springs with small damping. The mechanical model of the drivetrain follows from Figure 1. Here, j_i represents the inertias of the drivetrain, c_i the stiffnesses and φ_i the degrees of freedom. The parameters u_3 and u_6 represent the gear ratio and the final drive ratio. T_{eng} represents the engine torque, which is applied to the crankshaft j_2.
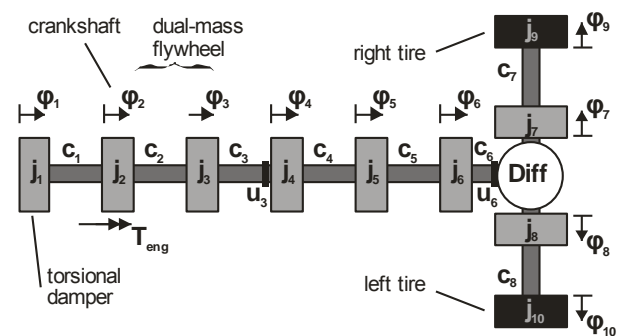
Figure 1: Mechanical Drivetrain System

Tires are implemented as elements that calculate the force between wheel and street according to the differential speed of both. Data for tires are usually measured with a dedicated tire rig and implemented via a curve fitting algorithm. The longitudinal tire force follows according to (Pacejka and Bakker 1992):

$$F_{tire} = s \cdot \beta(F_{load}^{tire}) \tag{3}$$

$$s = \frac{r_{tire} \cdot w_{tire} - v_{vehicle}}{r_{tire} \cdot w_{tire}} \tag{4}$$

Here, r_{tire} represents the tire radius, w_{tire} the tire rotational speed and $v_{vehicle}$ the vehicle speed. The tire load F_{load}^{tire} of the rear tire is calculated according to the balance of momentum of the accelerated vehicle, as illustrated in Figure 2. The variable $F_{gravity}$ represents the mass force due to gravity, h represents the height of the centre of mass of the vehicle and l_f and l_r the horizontal distance between front and rear wheel contact point to the centre of mass of the vehicle. The balance of momentum at the front wheel contact point calculates the rear axle load F_{load}^{rear} and thus the tire load according to:

$$F_{load}^{rear} = \frac{F_{tire}\,h + F_{gravity}\,l_f}{l_f + l_r} = 2\,F_{load}^{tire} \tag{5}$$
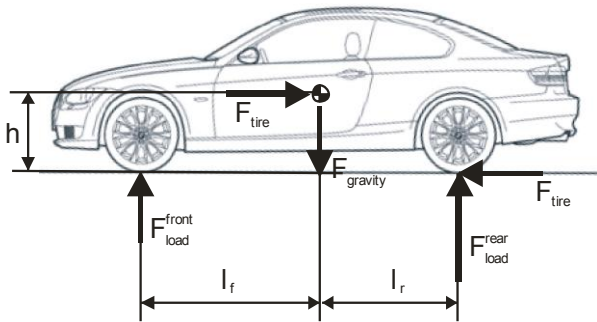
Figure 2: Vehicle Balance of Momentum

Tire force is a quantity proportional to differential speed s, so it can also be seen as non-linear damper with high damping coefficient. The function β represents the curve fitting algorithm, as shown in (Pacejka and Bakker 1992). The tire models illustrated in Figure 1 also contain an inertia that represents the rims.

The equations for the differential follow according to:

$$T_{in} = \frac{T_{out}^{right}}{2} = \frac{T_{out}^{left}}{2} \tag{6}$$

$$w_{in} = \frac{w_{out}^{right} + w_{out}^{left}}{2} \tag{7}$$

Here, T_{in} represents the torque of the input shaft and T_{out}^{right} and T_{out}^{left} of the right and left output shaft. Furthermore, w_{in} represents the rotational speed of the input shaft and w_{out}^{right} and w_{out}^{left} of the right and left output shaft of the differential. The parameters for all shafts and additional compliant elements are measured on component rigs. All inertias are corrected according to the gear ratio for the equivalent degree of freedom.

2.3. Measurement Comparison

In order to verify the correctness of the drivetrain model, an accurate measurement comparison is required. Therefore, a Tip-In manoeuvre was measured, i.e. the acceleration pedal of a prototype vehicle with constant speed is quickly acted from a defined part load throttle to full throttle. The first gear is engaged here.

The measurement results and the corresponding simulations for the vehicle are illustrated in the following figures. Figure 3 illustrates the intake manifold pressure, which is derived from a dedicated pressure sensor. For the simulated and measured manoeuvre, the acceleration pedal is acted at $t = 0.5\,\text{s}$. The figure shows that there is good consistence for the intake manifold pressure between measurement and simulation.
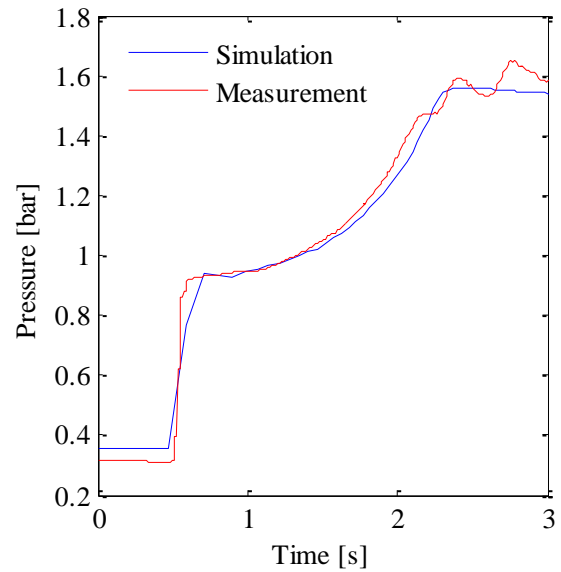
Figure 3: Measurement Comparison of the Intake Manifold Pressure

Figure 4 illustrates the engine torque. The measured engine torque is actually derived from an engine model on the engine control unit (ECU), which estimates the current torque according to diverse measured data, e.g. crankshaft speed or the intake manifold pressure. Apparently, there is also good consistence between measured and simulated engine torque. The first rise of the engine torque is very steep and results in an excitation that is similar to a torque step function. This occurs because of the rapid filling of the intake manifold and the cylinders after increasing the throttle diameter and the subsequent conversion into mechanical work by combusting a larger mass of air

and fuel. The following rise of the engine torque is a consequence of the turbocharger, which has a certain time delay because of its inertia.
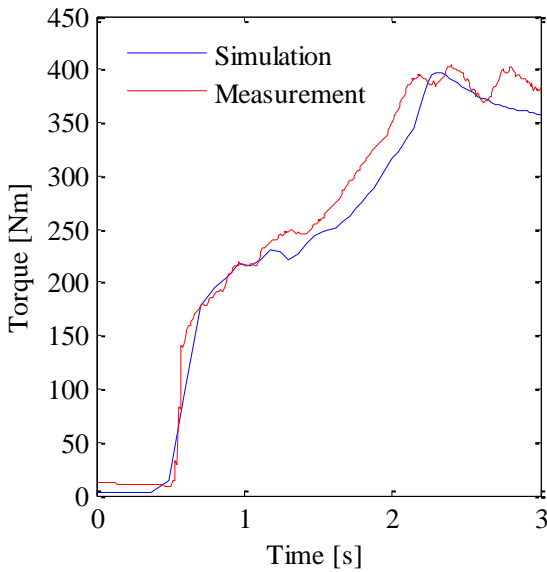
Figure 4: Measurement Comparison of the Engine Torque

A measure comparison for the mechanical drivetrain is also required, as follows in Figure 5. Here, the drivetrain model is acted by the measured engine torque. The longitudinal acceleration of the vehicle is illustrated. The drivetrain model shows good consistence between measurements and simulation. Note that several control algorithms for the damping of oscillations within the ECU are not considered here and were switched off for the measurements to avoid masking the drivetrain behaviour with interference of these algorithm interactions for examined frequencies.
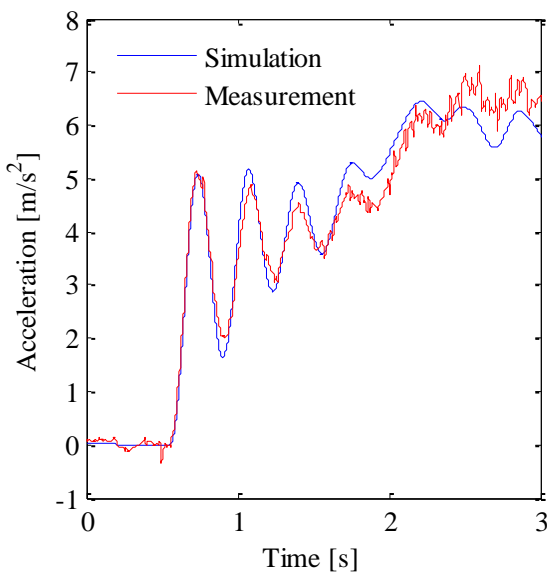
Figure 5: Measurement Comparison of the Vehicle Acceleration

3. DESIRED VEHICLE BEHAVIOUR

Figure 5 illustrates the vehicle longitudinal acceleration for a Tip-In manoeuvre. The excitation of the drivetrain via the engine similar to a step function results in a dominant stimulus of the first eigenfrequency with approximately 2.5 Hz for the vehicle longitudinal acceleration.

In fact, also higher eigenfrequencies of the drivetrain are stimulated by the step excitation. Nevertheless, for higher frequencies less energy is brought into the system for a step function excitation, higher frequencies oscillate with smaller magnitudes and they are quickly damped due to their higher rotational velocity. These effects explain the dominance of the first eigenfrequency for the vehicle longitudinal acceleration.

The desired vehicle behaviour is described from a driver perspective. For the discussed Tip-In manoeuvre, a driver experiences oscillation of the longitudinal vehicle acceleration, also referred to as shuffle, buckling or Bonanza effect, as perturbing. Particularly the height of the oscillation amplitudes is considerable to the driver. The frequency of this oscillation on the other hand is of less importance. Shuffle oscillations are usually between 2-5 Hz and in fact it is difficult for the driver to resolve a difference between these low frequencies. A quick decline of the oscillation is of higher importance. Additionally, the driver appreciates a steep rise in the vehicle acceleration curve.

For a higher frequency of the first drivetrain eigenfrequency, the oscillation amplitude is lower, the damping effect is stronger and the acceleration curve is steeper. As a result, a driver prefers higher frequencies for the first eigenfrequency of the vehicle drivetrain.

From this point of view, a consequence for the vehicle drivetrain design could be to choose e.g. shafts with high stiffness in order to move the first eigenfrequency to higher frequencies. This perspective however is too narrow for a drivetrain design. Driving a vehicle in other use cases also results in exciting higher drivetrain frequencies. In particular for drivetrains with three or even less cylinder engines, the second eigenfrequency is excited by the cyclic irregularity of the engine during stationary operation for low engine speeds $n < 1,500$ rpm in 5th or 6th gear. For higher engine speed or engines with more cylinders, the cyclic irregularity of the engine is also a problem, but the oscillations are transferred to the driver with smaller amplitudes. For these oscillation phenomena, other effects than the eigenfrequency affect the comfort perception of the driver as well. These aspects are not examined here. The focus of this paper is shuffle and cyclic irregularity due to excitation of drivetrain eigenfrequencies.

Even though shuffle and cyclic irregularity are examined with different gears, they illustrate a serious conflict of objectives for the vehicle drivetrain design. A simple optimization of shuffle, e.g. choosing stiffer shafts, would result in a higher frequency of the first and second eigenfrequency of the drivetrain. A higher

second eigenfrequency however is then closer or identical to the cyclic irregularity of the engine for certain vehicle speeds. Vice versa, a simple optimization of the cyclic irregularity behaviour could worsen shuffle. An efficient drivetrain design therefore must take both effects into account and resolve this conflict of objectives.

4. SENSITIVITY ANALYSIS

The eigenfrequency methodology is presented in this section. First, simplifications of the drivetrain model are performed, followed by the application of the sensitivity analysis based on (Dresig and Holzweißig 2010). Subsequently, palliative measures are derived and examined with the detailed model.

4.1. Simplifications

In order to examine the eigenfrequencies, simplifications are performed here. The thermodynamic engine model is of less interest since it essentially defines the excitation, the interaction is negligible. The crank drive is simplified as part of the crankshaft inertia. An additional simplification is concerned with the tire inertia and the vehicle mass. In relation to the drivetrain inertia, the vehicle mass is very high. Therefore the error caused by attaching the vehicle mass to the inertial frame is small. Furthermore, the tires are neglected and the rims are also fixed to the inertial frame. Due to the fact that there is generally only low damping for the drivetrain, damping effects are neglected for the sensitivity analysis. These simplifications actually influence the eigenfrequencies of the drivetrain and therefore a final comparison of the simplified model with the detailed drivetrain model is required.

The simplified drivetrain model is a one dimensional chain of inertias and springs:

$$M \ddot{x} + C x = 0 \qquad (8)$$

Here, x represents the vector for the rotational positions and $\ddot{x}$ the vector for the rotational accelerations of the inertias. The matrix of stiffness C follows according to:

$$C = \begin{bmatrix} c_1 & -c_1 & 0 & 0 & 0 & 0 & 0 & 0 \\ -c_1 & c_1+c_2 & -c_2 & 0 & 0 & 0 & 0 & 0 \\ 0 & -c_2 & c_2+c_3 & -u_3 c_3 & 0 & 0 & 0 & 0 \\ 0 & 0 & -u_3 c_3 & u_3^2 c_3+c_4 & -c_4 & 0 & 0 & 0 \\ 0 & 0 & 0 & -c_4 & c_4+c_5 & -c_5 & 0 & 0 \\ 0 & 0 & 0 & 0 & -c_5 & c_5+c_6 & -\frac{u_6}{2}c_6 & -\frac{u_6}{2}c_6 \\ 0 & 0 & 0 & 0 & 0 & -\frac{u_6}{2}c_6 & \frac{u_6^2}{4}c_6+c_7 & \frac{u_6^2}{4}c_6 \\ 0 & 0 & 0 & 0 & 0 & -\frac{u_6}{2}c_6 & \frac{u_6^2}{4}c_6 & \frac{u_6^2}{4}c_6+c_8 \end{bmatrix} \qquad (9)$$

The matrix of inertia M is diagonal according to:

$$M = \mathrm{diag}(j_1, j_2, j_3, j_4, j_5, j_6, j_7, j_8) \qquad (10)$$

There are only small deviations between the two models of first and fifth gear, e.g. gearing stiffness c_3 or gearing ratio u_3. The simplified model is illustrated in Figure 6.
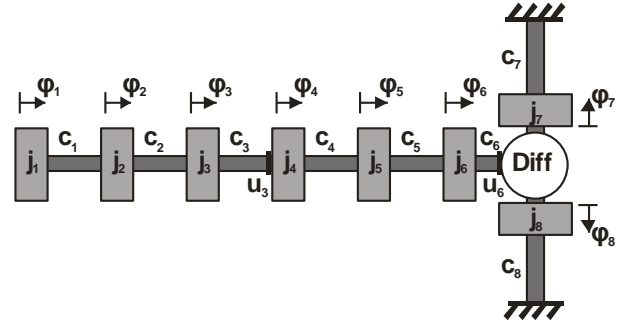
Figure 6: Reduced Mechanical Drivetrain Model

4.2. Sensitivity Algorithm

The presented sensitivity algorithm is based on (Dresig and Holzweißig 2010). A modal decomposition of the differential equation system of Equation (8) returns the modal inertia μ_i and stiffness γ_i as follows (Ulbrich 1996):

$$\gamma_i = v_i^T \cdot C \cdot v_i \qquad (11)$$

$$\mu_i = v_i^T \cdot M \cdot v_i \qquad (12)$$

Here, v_i represents the eigenvector of the eigenfrequency ω_i. The eigenfrequency ω_i is then calculated according to:

$$\omega_i^2 = \frac{\gamma_i}{\mu_i} = \frac{v_i^T \cdot C \cdot v_i}{v_i^T \cdot M \cdot v_i} \qquad (13)$$

Small variations of the inertias ΔM or the stiffnesses ΔC lead to small variations of the eigenfrequency $\Delta \omega_i$, and the change of the eigenvector is negligible $\Delta v_i \approx 0$:

$$\tilde{\omega}_i^2 = \omega_i^2 + \Delta \omega_i^2 = \frac{v_i^T \cdot (C+\Delta C) \cdot v_i}{v_i^T \cdot (M+\Delta M) \cdot v_i} \qquad (14)$$

Assuming that variations of the inertias are much smaller than the inertias themselves $\Delta M \ll M$, and $\Delta \omega_i$ can be estimated after some transposition according to (Dresig and Holzweißig 2010):

$$\Delta \omega_i^2 \approx \omega_i^2 \left(\frac{v_i^T \cdot \Delta C \cdot v_i}{v_i^T \cdot C \cdot v_i} - \frac{v_i^T \cdot \Delta M \cdot v_i}{v_i^T \cdot M \cdot v_i} \right) \qquad (15)$$

The variation matrices for stiffness ΔC and inertias ΔM are a sum of the variations of all inertias Δj_l and stiffnesses Δc_k:

$$\Delta M = \sum_l M_{l0} \cdot \frac{\Delta j_l}{j_l} \tag{16}$$

$$\Delta C = \sum_k C_{k0} \cdot \frac{\Delta c_k}{c_k} \tag{17}$$

The matrices C_{k0} and M_{l0} represent the introduced matrices for stiffness and inertias with all elements equal to zero, except element k or l respectively, e.g. for the inertias:

$$M_{l0} = \mathrm{diag}(0, \ldots, 0, j_l, 0, \ldots, 0) \tag{18}$$

This finally leads to the following sensitivity coefficients for stiffness φ_{ki} and inertia κ_{li} for eigenfrequency ω_i of element k or l respectively:

$$\Delta \omega_i^2 \approx \omega_i^2 \left(\sum_k \varphi_{ki} \cdot \frac{\Delta c_k}{c_k} - \sum_l \kappa_{li} \cdot \frac{\Delta j_l}{j_l} \right) \tag{19}$$

$$\varphi_{ki} = \frac{v_i^T \cdot C_{k0} \cdot v_i}{v_i^T \cdot C \cdot v_i} \tag{20}$$

$$\kappa_{li} = \frac{v_i^T \cdot M_{l0} \cdot v_i}{v_i^T \cdot M \cdot v_i} \tag{21}$$

These coefficients describe the variation of the eigenfrequency for a small relative parameter variation. Thus they are regarded as sensitivity coefficients for that eigenfrequency.

4.3. Drivetrain Eigenfrequency Analysis

For the presented drivetrain models for the first eigenfrequency of the first gear and the second eigenfrequency of the fifth gear, the sensitivity coefficients are illustrated in the following figures.

In order to solve the discussed conflict of objectives, the task now is to move the first eigenfrequency of the first gear to higher frequencies and vice versa move the second eigenfrequency of the fifth gear to lower frequencies. For a spring and mass system, an eigenfrequency is moved to higher frequencies by decreasing inertias or increasing stiffnesses, compare Equation (19). Figure 7 illustrates the sensitivity coefficients of the inertias and Figure 8 those of the stiffnesses for shuffle. The shuffle eigenfrequency is $\omega_1 = 2.5 \, \mathrm{Hz}$.
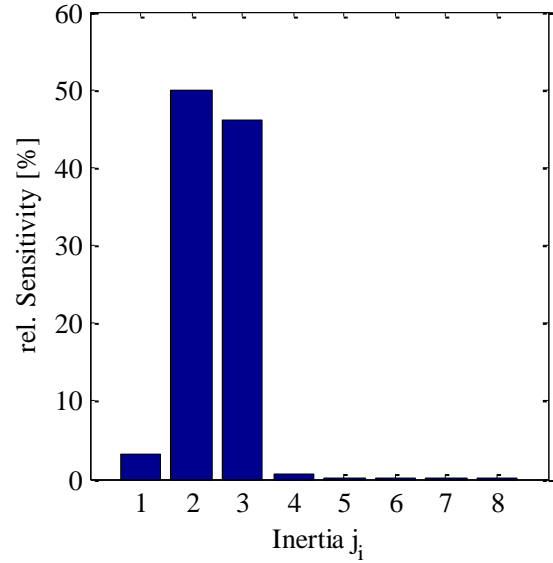
Figure 7: Sensitivity of Inertias for Shuffle
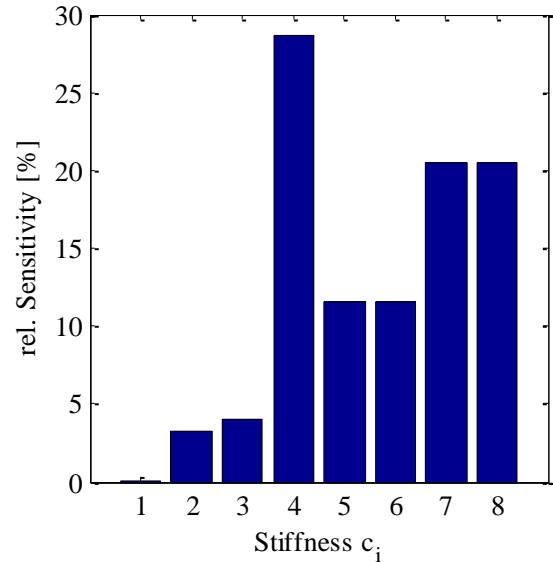
Figure 8: Sensitivity of Stiffnesses for Shuffle

For the shuffle eigenfrequency, there is a high sensitivity for the crankshaft inertia and the inertia of the dual-mass flywheel j_2 and j_3. Furthermore, there is a high sensitivity for the rubber joint and the sideshaft stiffness c_4, c_7 and c_8.

The same sensitivity analysis was performed for the relevant eigenfrequency for cyclic irregularity $\omega_2 = 17.1 \, \mathrm{Hz}$, as illustrated in Figure 9 for the inertias and Figure 10 for the stiffnesses.
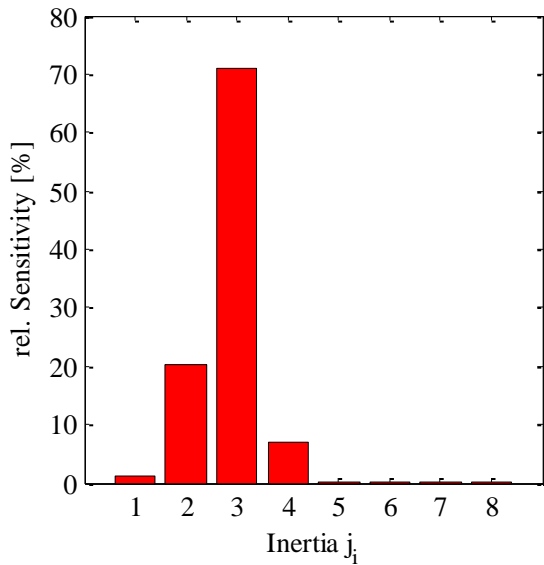
Figure 9: Sensitivity of Inertias for Cyclic Irregularity
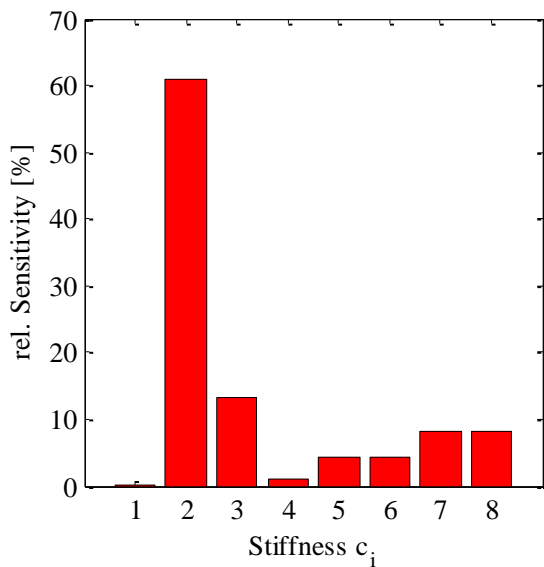
Figure 10: Sensitivity of Stiffnesses for Cyclic Irregularity

Figure 9 illustrates that there is a high sensitivity of the eigenfrequency for cyclic irregularity for the secondary mass of the dual-mass flywheel j_3. Furthermore, the stiffness of the dual-mass flywheel c_2 also shows high sensitivity for that eigenfrequency.

With the presented diagrams, it is now possible to identify combinations that raise the first eigenfrequency and decrease the second eigenfrequency as well. In order to derive a parameter combination as palliation measure, a first parameter is selected from the illustrations, which has a high sensitivity for shuffle and a low sensitivity for cyclic irregularity. Additionally, a second parameter is chosen with low sensitivity for shuffle and high sensitivity for cyclic irregularity.

4.4. Modifications of the Mechanical Drivetrain
Two different combinations will be discussed in the following section in order to illustrate the methodology

principle. From Figure 8 and Figure 10 it is apparent that the stiffness c_7, i.e. the stiffness of the right sideshaft, has a major influence on the shuffle eigenfrequency and a minor influence on the eigenfrequency of cyclic irregularity. On the other hand, stiffness c_2, i.e. the stiffness of the dual-mass flywheel, has a minor influence on the shuffle eigenfrequency and a major influence on the eigenfrequency of cyclic irregularity. A promising combination to solve the conflict of objectives could now be to increase stiffness c_7 and decrease stiffness c_2. In order to contain the symmetry of the drivetrain, stiffness c_8, i.e. the stiffness of the left sideshaft, also needs to be modified according to stiffness c_7. Here, the stiffnesses of the driveshafts are doubled and the stiffness of the dual-mass flywheel decreased to half of the original value. This results in modification 1:

$$c_2^{\mathrm{mod1}} = 0.5\,c_2 \tag{22a}$$

$$c_7^{\mathrm{mod1}} = 2\,c_7 \tag{22b}$$

$$c_8^{\mathrm{mod1}} = c_7^{\mathrm{mod1}} \tag{22c}$$

Additionally, another modification is examined to ensure that modification 1 is not a coincidence. The new parameter setup is referred to as modification 2:

$$c_4^{\mathrm{mod2}} = 2\,c_4 \tag{23a}$$

$$c_7^{\mathrm{mod2}} = 0.8\,c_7 \tag{23b}$$

$$c_8^{\mathrm{mod2}} = c_7^{\mathrm{mod2}} \tag{23c}$$
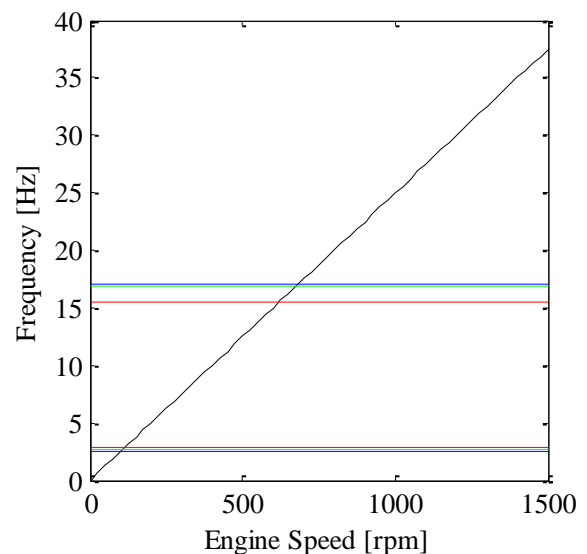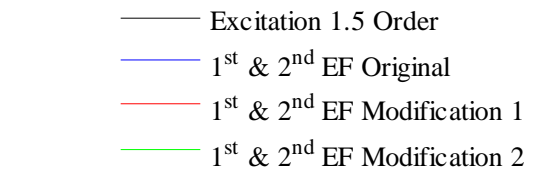
Figure 11: Campbell Diagram

The values for the parameter variation are derived so that the effect of one measure does not overcompensate the effect of the other. The Campbell diagram in Figure 11 shows the result of the drivetrain eigenfrequencies (EF) for both modifications.

The shuffle eigenfrequency of modification 1 is $\omega_1^{mod1} = 2.8\,\text{Hz}$, the eigenfrequency for cyclic irregularity is $\omega_2^{mod1} = 15.5\,\text{Hz}$. Furthermore, the shuffle eigenfrequency of modification 2 is $\omega_1^{mod2} = 2.6\,\text{Hz}$, the eigenfrequency for cyclic irregularity is $\omega_2^{mod2} = 16.9\,\text{Hz}$. Obviously, the aimed task to move both eigenfrequencies in the desired directions worked for both modifications. A weakness of the described methodology is the difficulty in predicting the precise frequency of the eigenfrequency of the new setup. Hence, the methodology helps to identify, which parameters should be modified in which direction, but not how high the parameter variation should be.

4.5. Simulative Measure Verification

Due to the performed simplifications it is finally required that the results also persist for the detailed model. The eigenfrequency of cyclic irregularity as examined here for low frequencies is a problem for the vehicle drivetrain because it is close to the excitation of the engine. For a three cylinder engine, it is particularly difficult since it excites the drivetrain with the 1.5 order. The excitation of a three cylinder engine is also illustrated in Figure 11. A detailed three cylinder model is derived in this work from the presented six cylinder model of section 2. Therefore, three cylinders are removed and additional modifications for the exhaust and the intake manifold are performed to generate the three cylinder model. In particular, parts of the exhaust and intake manifold system with two parallel paths of the six cylinder model are removed. Those parts with one common path are physically divided in half, e.g. the throttle cross section or the intake manifold volume. This model is used to obtain a realistic engine excitation.

Figure 12 illustrates the engine torque of the model for a Tip-In manoeuvre. This diagram shows that the three cylinder engine has a comparable steepness of the first torque raise which is followed by an engine torque which is approximately half as high as the six cylinder engine.

In Figure 13 the acceleration of the vehicle model is illustrated. Here, the original drivetrain model is excited with the three cylinder torque of Figure 12. Furthermore, the drivetrain model modification 1 is also excited by this engine torque. First remark is that due to the lower torque the absolute values of the acceleration and its oscillations are lower than those of the drivetrain of Section 2. Nevertheless, since the oscillations are observed in relation to the mean acceleration, the oscillations are still a problem.
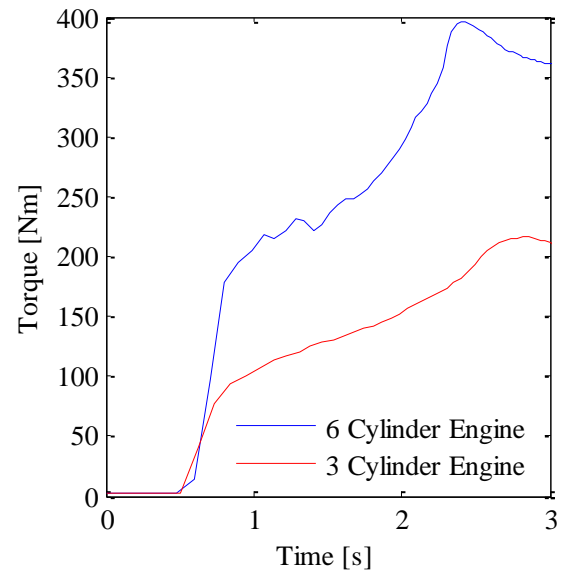
Figure 12: Engine Torque for Original and 3 Cylinder Engine

Additionally, Figure 13 shows that the aimed increase of the shuffle eigenfrequency worked for modification 1. Consequently, also the amplitude of the oscillations is reduced and the suggested measure worked for the simulation of shuffle as expected.
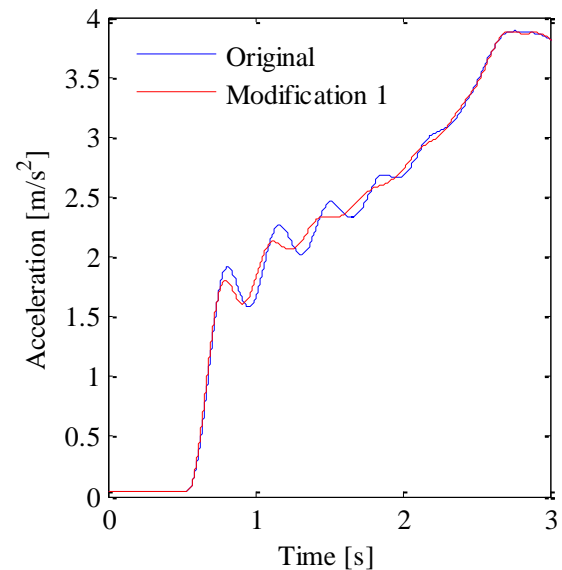
Figure 13: Vehicle Acceleration with Modification 1

Next step is the simulation of cyclic irregularity. Here, the three cylinder engine is again used to generate the excitation. For cyclic irregularity, a constant excitation for a dedicated engine speed is required. According to Figure 11, a low engine speed results in an excitation close to the eigenfrequency. For that reason $n = 1{,}000$ rpm is used as excitation. Figure 14 illustrates the torque acting on a distinct drivetrain shaft, which is relevant for cyclic irregularity, for the original drivetrain and the drivetrain modification 1 in order to evaluate oscillations due to cyclic irregularity.
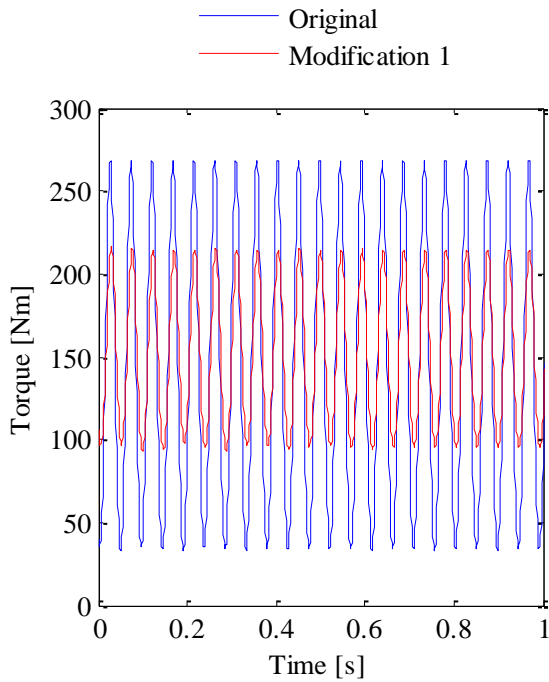
Figure 14: Cyclic Irregularity for n = 1,000 rpm, Modification 1

The illustration shows that the amplitude of the torque oscillation of the modified drivetrain decreased from 70 Nm to 30 Nm. Thus, the exemplary system modification worked in the desired way and helped to palliate the conflict of objectives between shuffle and cyclic irregularity.

For modification 2, the drivetrain was excited in the same way as described for modification 1 above. Figure 15 and Figure 16 illustrate the simulation results for drivetrain modification 2.
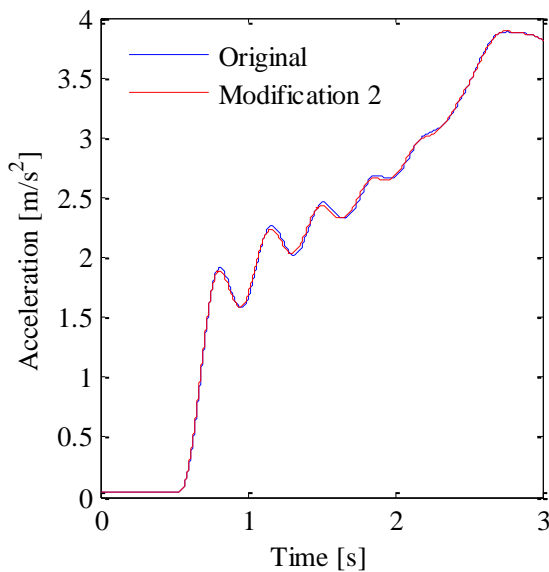
Figure 15: Vehicle Acceleration with Modification 2
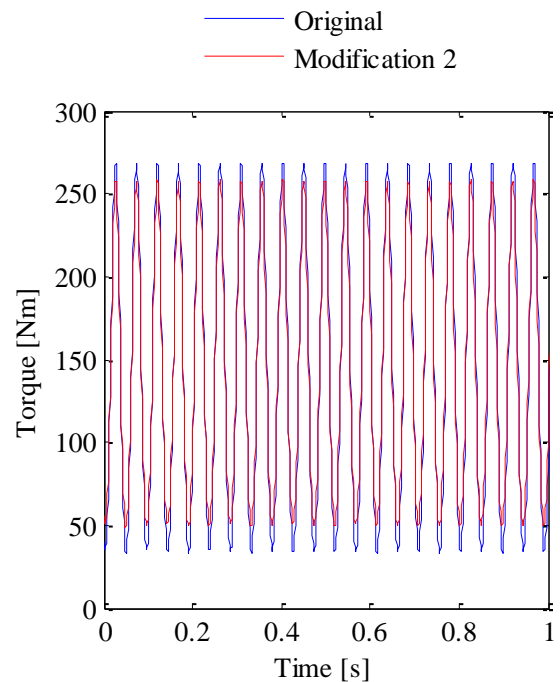
Figure 16: Cyclic Irregularity for n = 1,000 rpm, Modification 2

The vehicle acceleration in Figure 15 shows that the effect of modification 2 for shuffle is marginal. The reason for that is the minimal change of ω_1^{mod2}. The decrease of the first stiffness almost completely compensates the increase of the second stiffness. Improved behaviour is observable for cyclic irregularity in Figure 16. The effect of modification 2 is smaller than that of modification 1.

5. CONCLUSION

For vehicle drivetrain design, oscillations represent a major aspect in order to gain a setup that meets the comfort requirements of the driver. Shuffle and cyclic irregularities due to the engine excitation cause a serious conflict of objectives. A methodology is presented that can help to solve this conflict of objectives for selected drivetrain setups, based on an understanding of the drivetrain eigenfrequency sensitivities.

First, a detailed model of the drivetrain is presented in Section 2, containing a complex engine model for the vehicle excitation and a mechanical drivetrain model including tires. A measurement comparison for the engine torque, intake manifold pressure and the vehicle acceleration is presented to verify the correctness of the models. In Section 3, the desired vehicle behaviour and the conflict of objectives for the palliation of shuffle and cyclic irregularity is described. The methodology is presented in Section 4, starting with a simplification of the drivetrain model and an eigenfrequency sensitivity analysis based on (Dresig and Holzweißig 2010). The following visualisation facilitates the identification of palliation measures for the described conflict of objectives. Two exemplary palliation measures are

derived from these illustrations. In order to show the conflict of objectives, a three cylinder engine is derived from the examined models, which particularly suffers from the described conflict, since the excitation frequency is close to the second drivetrain eigenfrequency for low engine speed. The setup of the mechanical drivetrain is not changed any further to illustrate the methodology principle. Simulations for the detailed models show that the suggested, exemplary measures can palliate the described conflict of objectives for the observed drivetrain.

The example shows improved vehicle behaviour for the performed time-based simulations. Nevertheless, a final measurement comparison is required. It must eventually be clarified for other conditions of use that the suggested measures will not worsen the vehicle behaviour for those use cases. This can also include oscillations of cyclic irregularity for higher frequencies since other effects affect the driver perception here as well.

It shall also be remarked that the described method is not the usual method to derive a drivetrain setup. In particular, the vehicle mass of the three cylinder engine remained identical to the six cylinder engine. Also the gear and final drive ratios remained the same. For a drivetrain design in the industry, the gear and final drive ratio, the vehicle mass and additional parameters are adjusted to achieve a coherent vehicle setup. In this paper, these adoptions are neglected in order to demonstrate the methodology principle. It is the dedicated objective of the presented method to palliate the conflict of objectives between shuffle and cyclic irregularity and not to derive a drivetrain setup for new vehicle concepts.

Despite to an optimisation algorithm, the comparison of the sensitivities for the different use cases provides a profound understanding of the dynamic vehicle drivetrain behaviour. Furthermore, optimisation algorithms require distinct optimisation criteria and boundaries that often do not exist explicitly. In particular, for the heterogeneous design process of a vehicle with different responsibilities spread around research and development departments, a methodology providing a profound understanding of the dynamic behaviour is superior compared to a singular optimum.

REFERENCES

Baines, N., Fredriksson, C., 2007. The Simulation of Turbocharger Performance for Engine Matching. In: Pucher, ed., H., Kahrstedt, J., ed. *Motorprozesssimulation und Aufladung 2: Engine Process Simulation and Supercharging*. Expert, Berlin: pp. 101-111.

Bencker, R., 1998. *Simulationstechnische und experimentelle Untersuchung von Lastwechsel-phänomenen an Fahrzeugen mit Standardantrieb*. Munich: Hieronymus.

Best, M.C., 1998. Nonlinear optimal control of vehicle driveline vibrations. *UKACC International Conference on Control ´98 (Conf. Publ. No. 455)*.

Dick, E., 2009. Introduction to Finite Volume Methods in Computational Fluid Dynamics. In: Wendt, J. F., ed. *Computational Fluid Dynamics*. Springer, Berlin: pp. 87-103.

Dresig, H., Holzweißig, F., 2010. *Dynamics of Machinery: Theory and Application*. Berlin: Springer.

Gosdin, M., 1985. *Analyse und Optimierung des dynamischen Verhaltens eines Pkw-Antriebsstranges*. Düsseldorf: VDI.

Hülsmann, A., 2007. *Methodenentwicklung zur virtuellen Auslegung von Lastwechselphänomenen in PKW*. Munich: Technische Universität München, Dissertation.

Krieg, O.M., Förg, M., Ulbrich, H., 2011. Simulation of Domain-Coupled Multibody and Thermodynamic Problems for Automotive Applications. *Proceedings of Multibody Dynamics 2011*. July 4-7, Brussels, Belgium.

Lefebvre, D., Chevrel, P., Richard, S., 2003. An H-Infinity-Based Control Design Methodology Dedicated to the Active Control of Vehicle Longitudinal Oscillations. *IEEE Transactions On Control Systems Technology,* Volume 11, No. 6: pp. 948-956.

Miersch, J., 2003. *Transiente Simulation zur Bewertung von ottomotorischen Konzepten*. Munich: Hieronymus.

Müller, I., Müller, W.H., 2005. *Fundamentals of Thermodynamics and Applications*. Berlin: Springer.

Pacejka, H.B., Bakker, E., 1992. The Magic Formula Tyre Model. *Vehicle System Dynamics: International Journal of Vehicle Mechanics and Mobility,* Volume 21, Issue S1: pp. 1-18.

Reik, W., Fidlin, A., Seebacher, R. 2009. Gute Schwingung – Böse Schwingung: *Proceedings of 6. VDI-Fachtagung Schwingungen in Antrieben:* pp. 3-15.

Richard, S., Chevrel, P., Maillard, B. 1999. Active Control of future vehicles drivelines. *Proceedings of the 38th Conference on Decision & Control:* pp. 3752-3757.

Ulbrich, H., 1996. *Maschinendynamik*. Wiesbaden: Teubner.